

# Parallel coupled and uncoupled multilevel solvers for the Bidomain model of electrocardiology

Piero Colli Franzone<sup>1</sup>, Luca F. Pavarino<sup>2</sup>, and Simone Scacchi<sup>2</sup>

## 1 Introduction

The Bidomain model describes the spread of electrical excitation in the anisotropic cardiac tissue in terms of the evolution of the transmembrane and extracellular electric potentials,  $v$  and  $u_e$  respectively. This model consists of a non-linear parabolic reaction-diffusion partial differential equation (PDE) for  $v$ , coupled with an elliptic linear PDE for  $u_e$ . The evolution equation is coupled through the non-linear reaction term with a stiff system of ordinary differential equations (ODEs), the so-called membrane model, describing the ionic currents through the cellular membrane. The different space and time scales involved make the solution of the Bidomain system a very challenging computational problem, because its discretization in three-dimensional ventricular geometries of realistic size requires the solution of large scale (often exceeding  $O(10^7)$  unknowns) and ill-conditioned linear systems at each time step.

Several approaches have been developed in order to reduce the high computational costs of the Bidomain model. Fully implicit methods in time, requiring the solution of non-linear systems at each time step, have been considered in e.g. [10, 9]. Alternatively, most previous works have considered IMEX time discretizations and/or operator splitting schemes, where the reaction and diffusion terms are treated separately, see e.g. [2, 3, 18, 20, 23]. The advantage of IMEX and operator splitting schemes is that they only require the solution of a linear system for the parabolic and elliptic PDEs at each time step. A further splitting approach consists in uncoupling the parabolic PDE from the elliptic one, see e.g. [23, 4].

Many different preconditioners have been proposed in order to obtain efficient iterative solvers for the linear systems deriving from both splitting and uncoupling techniques: block diagonal or triangular [13, 14, 2, 22, 5], optimized Schwarz [6], multigrid [19, 16, 15, 13, 14], multilevel Schwarz [11], Balancing Neumann-Neumann [24] and BDDC [25] preconditioners.

The aim of the present work is to apply the Multilevel Additive Schwarz preconditioners of [11] to both a coupled and an uncoupled time discretization of the Bidomain system and to compare their parallel performance. Three-dimensional parallel numerical tests on a BlueGene cluster, reported in Sec. 4, show that the uncou-

---

<sup>1</sup> Department of Mathematics, University of Pavia, via Ferrata 1, 27100 Pavia, Italy, e-mail: [colli@imati.cnr.it](mailto:colli@imati.cnr.it). <sup>2</sup> Department of Mathematics, University of Milano, via Saldini 50, 20133 Milano, Italy, e-mail: [{luca.pavarino}{simone.scacchi}@unimi.it](mailto:{luca.pavarino}{simone.scacchi}@unimi.it)

pled technique is as scalable as the coupled one. Moreover, the conjugate gradient method preconditioned by Multilevel Additive Schwarz preconditioners converges faster for the uncoupled system than for the coupled one. Finally, in all parallel numerical tests considered, the uncoupled technique proposed is always about 1.5 times faster than the coupled approach.

## 2 The anisotropic Bidomain model

The macroscopic Bidomain representation of the cardiac tissue volume  $\Omega$  is obtained by considering the superposition of two anisotropic continuous media, the intra- (i) and extra- (e) cellular media, coexisting at every point of the tissue and separated by a distributed continuous cellular membrane; see e.g. [12] for a derivation of the Bidomain model from homogenization of cellular models. We recall that the cardiac tissue consists of an arrangement of fibers that rotate counterclockwise from epi- to endocardium, and that have a laminar organization modeled as a set of muscle sheets running radially from epi- to endocardium, see [7]. The anisotropy of the intra- and extracellular media is described by the orthotropic conductivity tensors  $D_i(\mathbf{x})$  and  $D_e(\mathbf{x})$ , see e.g. [2].

We denote by  $\Omega \subset \mathbb{R}^3$  the bounded physical region occupied by the cardiac tissue and introduce a parabolic-elliptic formulation of the Bidomain system. Given an applied extracellular current per unit volume  $I_{app}^e : \Omega \times (0, T) \rightarrow \mathbb{R}$ , we seek the transmembrane potential  $v : \Omega \times (0, T) \rightarrow \mathbb{R}$ , extracellular potentials  $u_e : \Omega \times (0, T) \rightarrow \mathbb{R}$ , gating variables  $w : \Omega \times (0, T) \rightarrow \mathbb{R}^{N_w}$  and ionic concentrations  $c : \Omega \times (0, T) \rightarrow \mathbb{R}^{N_c}$  such that

$$\begin{cases} c_m \frac{\partial v}{\partial t} - \operatorname{div}(D_i(\mathbf{x})\nabla v) - \operatorname{div}(D_i(\mathbf{x})\nabla u_e) + I_{ion}(v, w, c) = 0 & \text{in } \Omega \times (0, T) \\ -\operatorname{div}(D_i(\mathbf{x})\nabla v) - \operatorname{div}((D_i(\mathbf{x}) + D_e(\mathbf{x}))\nabla u_e) = I_{app}^e & \text{in } \Omega \times (0, T) \\ \frac{\partial w}{\partial t} - R(v, w) = 0, \quad \frac{\partial c}{\partial t} - S(v, w, c) = 0, & \text{in } \Omega \times (0, T) \end{cases} \quad (1)$$

with insulating boundary conditions, suitable initial conditions on  $v, w, c$  and where  $c_m$  is the membrane capacitance per unit volume. The non-linear reaction term  $I_{ion}$  and the ODE system for the gating variables  $w$  and the ionic concentrations  $c$  are given by the chosen ionic membrane model. Here we will consider the Luo-Rudy I (LR1) membrane model [8].

## 3 Discretization and numerical methods

**Space discretization.** The variational formulation of system (1) is first discretized in space by the finite element method. In this work, we will consider isoparametric

trilinear finite elements on hexahedral meshes. In the following, we denote by  $A_{i,e}$  the symmetric intra- and extracellular stiffness matrices and by  $M$  the mass matrix. We define the block mass and stiffness matrices as

$$\mathbb{M} = \begin{bmatrix} M & 0 \\ 0 & 0 \end{bmatrix}, \quad \mathbb{A} = \begin{bmatrix} A_i & A_i \\ A_i & A_i + A_e \end{bmatrix}.$$

**Time discretization.** We consider two implicit-explicit (IMEX) strategies, both based on decoupling the ODEs from the PDEs and on treating the linear diffusion terms implicitly and the non-linear reaction terms explicitly.

- **Coupled method.** The equations arising from the discretization of the PDEs are solved as a coupled system. Given  $\mathbf{w}^n$ ,  $\mathbf{c}^n$ ,  $\mathbf{v}^n$ ,  $\mathbf{u}_e^n$  at the generic time step  $n$ :
  - we first solve the ODEs system using the Implicit Euler method for the gating variables and the Explicit Euler method for the ionic concentrations, obtaining the new gating variables  $\mathbf{w}^{n+1}$  and the new ionic concentrations  $\mathbf{c}^{n+1}$ ,
  - then we solve the PDEs system, obtaining the new potentials  $\mathbf{v}^{n+1}$  and  $\mathbf{u}_e^{n+1}$ .
 Summarizing in formulae, given  $\mathbf{w}^n$ ,  $\mathbf{c}^n$ ,  $\mathbf{v}^n$ ,  $\mathbf{u}_e^n$ , the scheme is

$$\begin{aligned} \mathbf{w}^{n+1} - \Delta t \mathbf{R}(\mathbf{v}^n, \mathbf{w}^{n+1}) &= \mathbf{w}^n \\ \mathbf{c}^{n+1} &= \mathbf{c}^n + \Delta t \mathbf{S}(\mathbf{v}^n, \mathbf{w}^{n+1}, \mathbf{c}^n) \\ \left( \frac{c_m}{\Delta t} \mathbb{M} + \mathbb{A} \right) \begin{bmatrix} \mathbf{v}^{n+1} \\ \mathbf{u}_e^{n+1} \end{bmatrix} &= \frac{c_m}{\Delta t} \mathbb{M} \begin{bmatrix} \mathbf{v}^n \\ \mathbf{u}_e^n \end{bmatrix} + \begin{bmatrix} -M\mathbf{I}_{ion}(\mathbf{v}^n, \mathbf{w}^{n+1}, \mathbf{c}^{n+1}) \\ M\mathbf{I}_{app}^{e,n+1} \end{bmatrix}. \end{aligned}$$

As a consequence, at each time step, we solve one linear system with unknowns  $(\mathbf{v}^{n+1}, \mathbf{u}_e^{n+1})$ . Because the iteration matrix is symmetric positive semi-definite, the iterative method employed is the preconditioned conjugate gradient (PCG) method. Due to the ill-conditioning of the iteration matrix and the large number of unknowns required by realistic simulations of cardiac excitation in three-dimensional domains, a scalable and efficient preconditioner is required. We adopt here the 4-level Multilevel Additive Schwarz (MAS(4)) preconditioner, see [21, 11].

- **Uncoupled method.** The two equations arising from the discretization of the PDEs are uncoupled by introducing the following scheme. Given  $\mathbf{w}^n$ ,  $\mathbf{c}^n$ ,  $\mathbf{v}^n$ ,  $\mathbf{u}_e^n$  at the generic time step  $n$ :
  - we first solve the ODEs system using the Implicit Euler method for the gating variables and the Explicit Euler method for the ionic concentrations, obtaining the new gating variables  $\mathbf{w}^{n+1}$  and the new ionic concentrations  $\mathbf{c}^{n+1}$ ,
  - then we solve the elliptic equation, obtaining  $\mathbf{u}_e^n$ ,
  - and finally we update the transmembrane potential  $\mathbf{v}^{n+1}$  by solving again the parabolic equation.
 Summarizing in formulae, given  $\mathbf{w}^n$ ,  $\mathbf{c}^n$ ,  $\mathbf{v}^n$ ,  $\mathbf{u}_e^n$ , the uncoupled scheme is

$$\begin{aligned}
\mathbf{w}^{n+1} - \Delta t \mathbf{R}(\mathbf{v}^n, \mathbf{w}^{n+1}) &= \mathbf{w}^n \\
\mathbf{c}^{n+1} &= \mathbf{c}^n + \Delta t \mathbf{S}(\mathbf{v}^n, \mathbf{w}^{n+1}, \mathbf{c}^n) \\
(A_i + A_e) \mathbf{u}_e^n &= -A_i \mathbf{v}^n + \mathbf{M} \mathbf{I}_{app}^{e,n} \\
\left( \frac{c_m}{\Delta t} M + A_i \right) \mathbf{v}^{n+1} &= \frac{c_m}{\Delta t} M \mathbf{v}^n - A_i \mathbf{u}_e^n - \mathbf{M} \mathbf{I}_{ion}(\mathbf{v}^n, \mathbf{w}^{n+1}, \mathbf{c}^{n+1}).
\end{aligned}$$

As a consequence, at each time step we solve first the linear system with matrix  $A_i + A_e$  deriving from the elliptic equation and afterwards the linear system with matrix  $\frac{c_m}{\Delta t} M + A_i$  deriving from the parabolic equation. Both linear systems are solved by the PCG method, since the matrices are symmetric positive definite in the parabolic case and semi-definite in the elliptic case. The preconditioner used for the parabolic system is Block Jacobi (BJ), because the related matrix is well-conditioned, while the preconditioner used for the ill-conditioned elliptic system is the MAS(4) preconditioner, described below.

**Multilevel Additive Schwarz preconditioners.** Let  $\Omega^k$ , for  $k = 0, \dots, \ell - 1$ , be a family of  $\ell$  nested triangulations of  $\Omega$ , coarsening from  $\ell - 1$  to 0,  $A^{\ell-1} = \mathbb{A}$  in the coupled method and  $A^{\ell-1} = A_i + A_e$  in the uncoupled method, and  $R^k$  the restriction operators from  $\Omega^{\ell-1}$  to  $\Omega^k$ . Define the matrices on each grid as  $A^k = R^k A^{\ell-1} R^{kT}$  for  $k = 0, \dots, \ell - 2$ . We then decompose each grid  $\Omega^k$ , for  $k = 1, \dots, \ell - 1$ , into  $N$  overlapping subgrids  $\Omega_m^k$  for  $m = 1, \dots, N$  and define the local restriction operators  $R_m^k$  from  $\Omega^{\ell-1}$  to  $\Omega_m^k$  and the local matrices  $A_m^k = R_m^k A^{\ell-1} R_m^{kT}$ . The Multilevel Additive Schwarz (MAS( $\ell$ )) preconditioner is given by

$$B_{MAS}^{-1} = R^{0T} A^{0-1} R^0 + \sum_{k=1}^{\ell-1} \sum_{m=1}^N R_m^{kT} A_m^{k-1} R_m^k.$$

The condition number of the resulting preconditioner operator  $T_{MAS} = B_{MAS}^{-1} A^{\ell-1}$  is bounded by

$$\kappa_2(T_{MAS}) \leq C \max_{k=1, \dots, \ell-1} \left( 1 + \frac{h_{k-1}}{\delta_k} \right),$$

where  $h_k$  is the mesh size of  $\Omega^k$  grid,  $\delta_k$  is the overlap size on level  $k$  and  $C$  is a constant independent of  $h_k$ ,  $\delta_k$ ,  $N$  and  $\ell$ ; see [11] and for hybrid variants [17].

## 4 Numerical results

In this section, we present the results of parallel numerical experiments performed on the BlueGene Cluster BG/Q of the Cineca Consortium ([www.cineca.it](http://www.cineca.it)). Our FORTRAN code is based on the parallel library PETSc [1], from the Argonne National Laboratory.

<i>procs</i>	<i>dof</i>	coupled			uncoupled		
		$\kappa_2 = \lambda_M/\lambda_m$	<i>it</i>	<i>time</i>	$\kappa_2 = \lambda_M/\lambda_m$	<i>it</i>	<i>time</i>
64	4,319,890	41.85=8.70/2.08e-1	43	5.65	15.52=4.50/2.90e-1	29	1.82+1.07=2.89
128	8,553,474	33.41=6.79/2.03e-1	39	5.57	14.94=4.46/2.99e-1	28	2.02+1.03=3.05
256	17,040,642	36.37=6.81/1.87e-1	40	5.70	15.36=4.46/2.91e-1	28	1.92+1.05=2.97
512	33,949,186	27.37=5.16/1.88e-1	36	5.48	14.35=4.38/3.05e-1	28	1.98+0.99=2.97
1,024	67,766,274	29.53=5.16/1.75e-1	36	5.69	14.43=4.42/3.06e-1	28	2.17+1.04=3.21
2,048	135,268,866	27.56=5.08/1.84e-1	34	8.50	13.23=4.33/3.28e-1	27	2.93+1.72=4.65
4,096	270,274,050	28.91=5.09/1.76e-1	34	16.39	13.23=4.33/3.28e-1	27	5.58+3.63=9.21
8,192	540,021,250	25.03=5.10/2.04e-1	32	16.51	12.41=4.30/3.47e-1	26	5.93+3.75=9.68
16,384	1,079,515,650	26.55=5.11/1.92e-1	32	17.39	12.41=4.30/3.47e-1	26	6.24+3.83=10.07
32,768	2,159,978,114	–	–	–	12.03=4.32/3.59e-1	26	6.90+3.94=10.84

**Table 1** Test 1. Weak scaling for coupled and uncoupled MAS(4) solvers on ellipsoidal structured meshes. Average condition number ( $\kappa_2$ ), extreme eigenvalues ( $\lambda_M, \lambda_m$ ), PCG iteration count (*it*) and CPU time in seconds (*time*) per time step. The CPU times in the uncoupled column are expressed as the sum of the elliptic plus the parabolic solver. The run with 32K cores in the case of coupled solver failed because of RAM limitations.

#### 4.1 Test 1: weak scaling on ellipsoidal domains, structured mesh

The coupled and uncoupled linear solvers are compared here in a scaled speedup test on ellipsoidal deformed domains, discretized by structured  $Q_1$  finite element grids. The number of subdomains (and processors) is increased from 64 to 32,768, forming increasing ellipsoidal domains  $\Omega$ . The fine mesh is chosen so as to keep the local mesh size on each subdomain fixed at  $32 \times 32 \times 32$ . With these choices, the global size of the discrete Bidomain system increases from about 4 million dof for the smallest domain with 64 subdomains to more than 2 billion dof for the largest domain with 32,768 subdomains. The physical dimensions of the increasing cartesian slabs are chosen so that the fine mesh size  $h$  is kept fixed to the value  $h = 0.01$  cm. The simulation is run for 10 time steps of 0.05 ms during the depolarization phase, which is the most intense computationally.

The results reported in Table 1 clearly show that, since the MAS(4) preconditioner is employed, both the coupled and uncoupled methods are scalable. In fact, all mathematical quantities (condition number, extreme eigenvalues, PCG iteration count) seem to approach constant values when increasing the number of subdomains. Also the CPU times scale quite well, because they only increase of about a factor 3 – 4 from 64 to 32,768 processors, with a very small and slow increase after 4096, while the global problem increases by a factor 512.

method	$it$	$Tit$	$time$	$Time$
coupled	22	82,861	2.43	9.29e+3
uncoupled	27	92,157	1.72	5.87e+3

**Table 2** Test 2. Comparison of coupled and uncoupled solvers on a whole heartbeat simulation, with 28,755,650 dof, 1,024 processors. Average PCG iteration count ( $it$ ) and CPU time ( $time$ ) per time step, total PCG iteration count ( $Tit$ ) and CPU time ( $Time$ ). The CPU times are expressed in seconds.

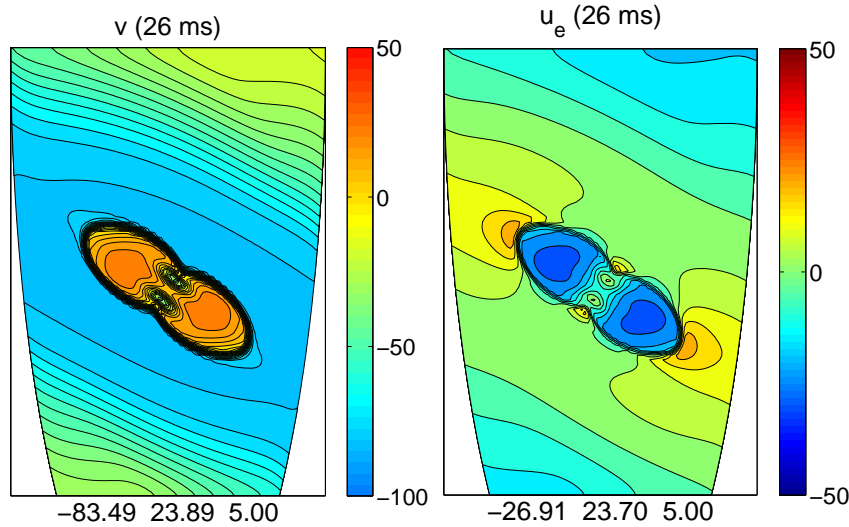


**Fig. 1** Test 2. Epicardial transmembrane (left) and extracellular (right) potential distributions at  $t = 26\text{ ms}$  after an electric stimulus applied during the systolic phase of the heart beat.

#### 4.2 Test 2: comparison between coupled and uncoupled methods on a complete cardiac cycle simulation

We now compare the coupled and uncoupled solvers on a complete heartbeat (500  $ms$ ) in a portion of an ellipsoid, modeling half of the left ventricle, discretized by a  $Q_1$  structured finite element grid of  $384 \times 384 \times 96$  elements (28,755,650  $dof$ ). The MAS(4) preconditioner is employed in the coupled solver and for the elliptic linear system in the uncoupled solver, while the BJ preconditioner is employed for the parabolic linear system in the uncoupled solver. The simulations are run on 1,024 cores. The time step size is changed according to the adaptive strategy described in [2].

The results reported in Table 2 show that the uncoupled method is about 1.5 times faster than the coupled one, because at each time step one solves two linear system of half size, the parabolic one being well conditioned and cheap to solve.

Fig. 1 reports the epicardial transmembrane and extracellular potential distributions at  $t = 26$  ms after an electric stimulus has been applied during the systolic phase of the heart beat at the center of the epicardial surface.

## 5 Conclusion

We have applied Multilevel Additive Schwarz preconditioners to both coupled and uncoupled time discretizations of the Bidomain model of the cardiac bioelectric activity and we have compared their parallel performance. Three-dimensional parallel numerical tests on a BlueGene/Q cluster up to 32K cores have shown that the uncoupled technique is as scalable as the coupled one. Moreover, the conjugate gradient method preconditioned by Multilevel Additive Schwarz preconditioners converges faster for the uncoupled system than for the coupled one. Finally, in all parallel numerical tests considered, the uncoupled technique proposed was always about 1.5 times faster than the coupled approach.

## References

1. Balay, S., et al.: PETSc users manual. Tech. Rep. ANL-95/11 - Revision 3.3, Argonne National Laboratory (2012)
2. Colli Franzone, P., Pavarino, L.F.: A parallel solver for reaction-diffusion systems in computational electrocardiology. *Math. Mod. Meth. Appl. Sci.* **14**, 883–911 (2004)
3. Ethier, M., Bourgault, Y.: Semi-implicit time-discretization schemes for the bidomain model. *SIAM J. Numer. Anal.* **46**, 2443–2468 (2008)
4. Fernandez, M.A., Zemzemi, N.: Decoupled time-marching schemes in computational cardiac electrophysiology. *Math. Biosci.* **226**, 58–75 (2010)
5. Gerardo Giorda, L., et al.: A model-based block-triangular preconditioner for the bidomain system in electrocardiology. *J. Comp. Phys.* **228**, 3625–3639 (2009)
6. Gerardo Giorda, L., et al.: Optimized Schwarz coupling of bidomain and monodomain models in electrocardiology. *Math. Model. Numer. Anal.* **45**, 309–334 (2011)
7. LeGrice, I.J., et al.: Laminar structure of the heart: ventricular myocyte arrangement and connective tissue architecture in the dog. *Am. J. Physiol. Heart Circ. Physiol.* **269**, H571–H582 (1995)
8. Luo, C., Rudy, Y.: A model of the ventricular cardiac action potential: depolarization, repolarization, and their interaction. *Circ. Res.* **68**, 1501–1526 (1991)
9. Munteanu, M., Pavarino, L.F., Scacchi, S.: A scalable Newton-Krylov-Schwarz method for the bidomain reaction-diffusion system. *SIAM J. Sci. Comput.* **31**, 3861–3883 (2009)
10. Murillo, M., Cai, X.C.: A fully implicit parallel algorithm for simulating the non-linear electrical activity of the heart. *Numer. Linear Algebra Appl.* **11**, 261–277 (2004)
11. Pavarino, L.F., Scacchi, S.: Multilevel additive Schwarz preconditioners for the Bidomain reaction-diffusion system. *SIAM J. Sci. Comput.* **31**, 420–443 (2008)
12. Pennacchio, M., Savaré, G., Colli Franzone, P.: Multiscale modeling for the bioelectric activity of the heart. *SIAM J. Math. Anal.* **37**, 1333–1370 (2006)
13. Pennacchio, M., Simoncini, V.: Algebraic multigrid preconditioners for the bidomain reaction-diffusion system. *Appl. Numer. Math.* **59**, 3033–3050 (2009)
14. Pennacchio, M., Simoncini, V.: Fast structured AMG preconditioning for the bidomain model in electrocardiology. *SIAM J. Sci. Comput.* **33**, 721–745 (2011)

15. Plank, G., et al.: Algebraic multigrid preconditioner for the cardiac bidomain model. *IEEE Trans. Biomed. Engrg.* **54**, 585–596 (2007)
16. Weber dos Santos, R., et al.: Parallel multigrid preconditioner for the cardiac bidomain model. *IEEE Trans. Biomed. Engrg.* **51**, 1960–1968 (2004)
17. Scacchi, S.: A hybrid multilevel Schwarz method for the bidomain model. *Comput. Meth. Appl. Mech. Engrg.* **197**, 4051–4061 (2008)
18. Southern, J.A., et al.: Solving the coupled system improves computational efficiency of the bidomain equations. *IEEE Trans. Biomed. Engrg.* **56**, 2404–2412 (2009)
19. Sundnes, J., et al.: Multigrid block preconditioning for a coupled system of partial differential equations modeling the electrical activity in the heart. *Comput. Meth. Biomech. Biomed. Engrg.* **5**, 397–409 (2002)
20. Sundnes, J., Lines, G.T., Tveito, A.: An operator splitting method for solving the bidomain equations coupled to a volume conductor model for the torso. *Math. Biosci.* **194**, 233–248 (2005)
21. Toselli, A., Widlund, O.B.: *Domain Decomposition Methods - Algorithms and Theory*. Springer-Verlag, Berlin (2004)
22. Vigmond, E.J., Aguel, F., Trayanova, N.A.: Computational techniques for solving the bidomain equations in three dimensions. *IEEE Trans. Biomed. Engrg.* **49**, 1260–1269 (2002)
23. Vigmond, E.J., et al.: Solvers for the cardiac bidomain equations. *Progr. Biophys. Molec. Biol.* **96**, 3–18 (2008)
24. Zampini, S.: Balancing Neumann-Neumann methods for the cardiac bidomain model. *Numer. Math.* **123**, 363–393 (2013)
25. Zampini, S.: Inexact BDDC methods for the cardiac bidomain model. In: *Proceedings of DD21* (2013)